Surface Chemistry

DOI: 10.1002/anie.201201533

Electrochemically Induced Surface-Initiated Atom-Transfer Radical Polymerization**

Bin Li, Bo Yu, Wilhelm T. S. Huck, Feng Zhou, and Weimin Liu*

Controlled/"living" surface-initiated radical polymerization offers the possibility to generate brushlike polymeric thin films with controllable thickness, composition, and architecture.[1,2] Polymer brushes have found widespread applications as model responsive[3,4] and non-biofouling surfaces,[5,6] in protein binding and immobilization studies,[7] chromatography supports,[8] in membrane applications,[9] antibacterial coatings,[10] actuation,[11,12] and low friction surfaces.[13,14] Among the many controlled polymerizations, atom-transfer radical polymerization (ATRP) is most widely used,[15] particularly for surface grafting in aqueous solution.[16–18] In standard surface-initiated ATRP, a Cu^I complex is used as the catalyst and high monomer concentrations are required to maximize the polymer growth. However, polymerization solutions often cannot be reused without purification, leading to inefficient use of the monomers. Furthermore, trace amount of oxygen will oxidize Cu^I to the deactivating Cu^{II} species and therefore, brush growth is usually carried out in an inert atmosphere. The conditions can be relaxed by employing advanced variations on ATRP as shown by Matyjaszewski et al.[19] Recently, the same group reported electrochemically mediated ATRP (eATRP) to control the polymerization of methacrylate monomers by a one-electron reduction of an initially added air-stable Cu^{II} salt.[20] Electrochemical generation of catalytically active Cu^I has been exploited in a surface "click" reaction between alkynes and azides.[21] Here, we report the controlled growth of polymer brushes under ambient conditions using surface-confined eATRP and the multiple reuse of the polymerization solution.

Scheme 1 shows the mechanism of polymer brush growth using eATRP. The reaction was carried out in an electrochemical cell with a three electrode system. A constant potential was applied to generate the Cu^ICl/bipyridine (bipy) complex through one-electron reduction of $Cu^{II}Cl_2$/bipy in the vicinity of initiator-decorated gold surface to initiate the polymerization. Prior to brush growth, cyclic voltammograms (CVs) of an initiator-modified electrode were carried out to identify the potential window for accurate manipulation of the reduction/oxidation state of the catalyst.[20] As shown in Figure 1a and 1b, no redox process occurred within the potential window from −0.6 to 0.3 V versus the saturated calomel electrode (SCE) when using ω-mercaptoundecyl bromoisobutyrate (SH-C15-Br)[22] decorated electrode because of the impedance of the monolayer to charge transfer.[23] The charge transfer resistance (R_{ct}) calculated from the electrical impedance spectrum of the surface is as large as 71 kΩ cm^2 (the R_{ct} of bare gold is only 6 Ω cm^2). When a shorter-chain alkanethiol initiator (2-mercaptoethyl-2-bromo-2-methylpropanoate, SH-C6-Br) modified electrode was used, a redox reaction occurred because of the low interfacial R_{ct} (1138 Ω cm^2, Figure 1b red curve and Table 1).

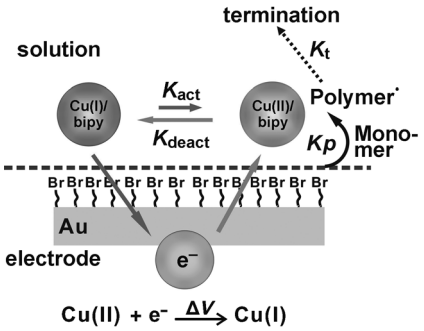

Scheme 1. Mechanism of electrochemically induced surface-initiated ATRP at a cathodic current to generate the Cu^ICl/bipy complex that triggers the polymerization (K_t = rate constant of chain termination, K_p = rate constants of chain propagation).

Table 1: The charge-transfer resistance (R_{ct}) and the calculated apparent electrode coverage (θ).

SAMs	SH-C_6-Br	SH-C_{15}-Br/2-NAT ratios in the stock solution					
		1:10	1:1	10:1	20:1	30:1	40:1
R_{ct}[Ω cm^2]	1138	623	2085	2470	4010	5273	31607
θ [%]	99.47	99.04	99.71	99.76	99.85	99.89	99.98

Short-chain alkanethiols are known for forming poorly packed self-assembled monolayers (SAMs) with pinhole defects, thus facilitating electron transfer.[24] It should therefore be possible to carry out eATRP using defect-rich SAMs at a reduction potential of approximately −0.31 V. During the experiments a color change at the interface because of the reduction of the deactivator $Cu^{II}Cl_2$/bipy complex to the activator Cu^ICl/bipy complex was observed. Unexpectedly, the polymer growth using SH-C6-Br SAMs is very limited

[*] B. Li, Dr. B. Yu, Prof. F. Zhou, Prof. W. Liu
State Key Laboratory of Solid Lubrication
Lanzhou Institute of Chemical Physics
Chinese Academy of Sciences, Lanzhou 730000 (China)
E-mail: zhouf@licp.cas.cn
Prof. W. T. S. Huck
Radboud University Nijmegen
Institute for Molecules and Materials
Heyendaalseweg 135, 6525 AJ Nijmegen (The Netherlands)

[**] Financial support from the NSFC (grant numbers 21125316 and 51171202) and the CAS (grant number KJZD-EW-M01).
Supporting information for this article is available on the WWW under http://dx.doi.org/10.1002/anie.201201533.

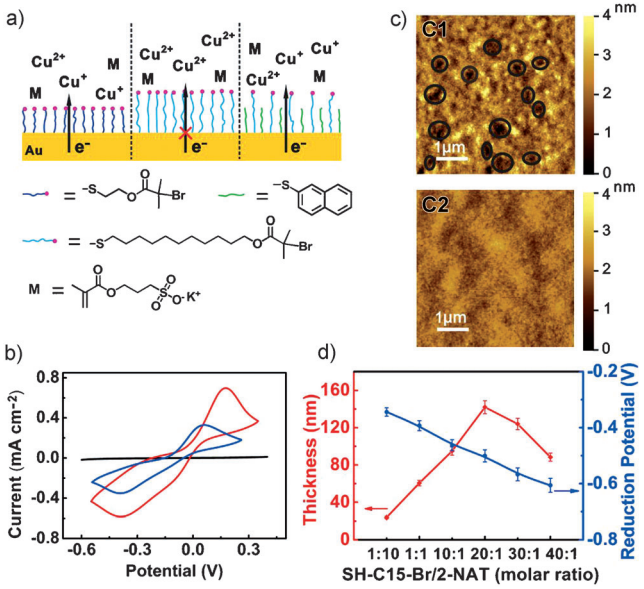

Figure 1. a) Electrochemically mediated ATRP on initiator-modified gold electrodes. b) Cyclic voltammograms of SH-C15-Br (dark curve), SH-C15-Br/2-NAT in a 1:1 ratio (blue curve), and a SH-C6-Br-modified electrode (area of 0.258 cm^2; red curve) in a SPMA monomer solution. c) AFM image of the morphology of PSPMA grown from SH-C6-Br (top) and SH-C15-Br/2-NAT (1:10; bottom) gold surfaces. d) The relationship of different SH-C15-Br/2NAT molar ratio, applied potential (blue curve), and PSPMA film thickness (red curve) grown on mixed monolayer surfaces (reaction time 2 h).

(only 18 nm thick PSPMA brushes were obtained after 2 h). The polymer films prepaired had a considerable amount of defects (Figure 1c, top) across the whole surface as detected by AFM.

To improve the brush growth and obtain smooth, homogeneous films, we formed mixed monolayers of 2-thionaphthiol (2-NAT) and SH-C15-Br. The X-ray photoelectron spectroscopy data (XPS, see Figure S1 in the Supporting Information) show the increase in the Br signal with increasing SH-C15-Br/2-NAT ratio. This strategy allowed us to not only create charge-transfer pathways for the redox reaction through 2-NAT domains (Figure 1a and 1c black line) but also to assemble high-quality initiator monolayers for the formation of dense polymer brushes. We found that both the applied potential and polymer growth were dependent on the relative fraction of SH-C15-Br and 2-NAT in the thiolate monolayers as shown in Table 1. The electron-transfer process in the mixed monolayer can be attributed to tunnelling mediated by a π-electron bridge.[25] For a blocked electrode, the charge-transfer resistance and the current density at an insulated electrode is inversely proportional to the thickness of insulation layer.[26] The surface coverage can be evaluated from the charge-transfer resistance according to Equation (1):[27]

$$(1-\theta) = R_{ct\circ}/R_{ct} \qquad (1)$$

where θ is the apparent electrode coverage, $R_{ct\circ}$ and R_{ct} are the charge-transfer resistance of bare electrode and the monolayer-covered electrode. Increasing the fraction of SH-C15-Br initiator, which forms a much more insulating SAM, resulted in a large increase in R_{ct} as the surface coverage approached one (Table 1).

Figure 1d shows the relationship between the reduction potential and polymer film thickness versus the SH-C15-Br/2-NAT ratios. Increasing the content of initiator in the stock solution leads to a negative shift in the potential used for eATRP and when the molar ratio of initiator to 2-NAT reaches 40:1 the reduction potential increased to −0.6, close to the reduction potential of Cu^0 (−0.7 V). The thickness of the polymer brushes is related to the density of the initiator sites as reported previously for mixed initiator monolayers.[28] However, polymer growth was limited at higher 2-NAT concentrations as the initiator fraction in the monolayer was too low. In all cases, polymer brushes grafted from mixed monolayers of SH-C15-Br/2-NAT = 1:10 showed a homogeneous morphology (Figure 1c, bottom), indicating a uniform distribution of SH-C15-Br in the mixed monolayers. The thickness of the polymer brushes increased with increasing SH-C15-Br/2-NAT ratio, to a maximum value of 142 nm in 2 h at a molar ratio of initiator to 2-NAT of 20:1. Beyond this ratio, the obtained thickness dropped as the resistance of the SAM increased leading to the generation of Cu^I ions.

We found that we can grow brushes using eATRP in the presence of air. We believe that any oxygen diffusing to the electrode surface is scavenged by Cu^I ions, which is then continuously regenerated. This relative insensitivity of the polymerization reaction for oxygen is similar to ARGET ATRP where deactivating Cu^{II} ions are reduced with appropriate reducing agents.[19] For the preparation of polymer brushes, this also means that the polymerization solution can be reused. Figure 2a shows that PSPMA brushes grown from Br-C15-thiol/2-NAT (20:1) electrodes in the same stock solution have almost the same thickness after 1 h in seven repeat experiments.

The polymerization rate in ATRP is determined by the relative concentration of Cu^I/Cu^{II} species and the corresponding equilibrium constant ($K_{eq} = k_{act}/k_{deact}$).[29] If K_{eq} is too large, the control is limited by the deactivation reaction and the propagating chains are liable to chain termination.[30] By adjusting the applied potential, we can control the amount of generated Cu^I ions, and so the ratio of Cu^I/Cu^{II}, and the number of activated chain ends.[31,32] Figure 2b shows the thickness as a function of the polymerization time at different applied potentials(Figure S3 in the Supporting information for current versus time curves). Polymer brush grow much faster at maximum reduction potential of −0.5 V than that at −0.35 V probably because of the rapidly generated Cu^I ions. At −0.5 V, the polymer brushes grow monotonously at first and level off after two hours, whereas the growth lasts longer at −0.35 V but the resulting thickness of the bushes is much lower. For polymerizations of one hour, the brush thickness obtained varied essentially linear with the applied potential. (Figure 2c), providing a new and externally controlled route to tailor the brush thickness. Other than surface-grafting polymerization at constant potentials, we also performed a polymerization by applying square-wave potentials. The polymer growth was initiated at a reducing potential and deactivated by applying a reverse positive potential with the

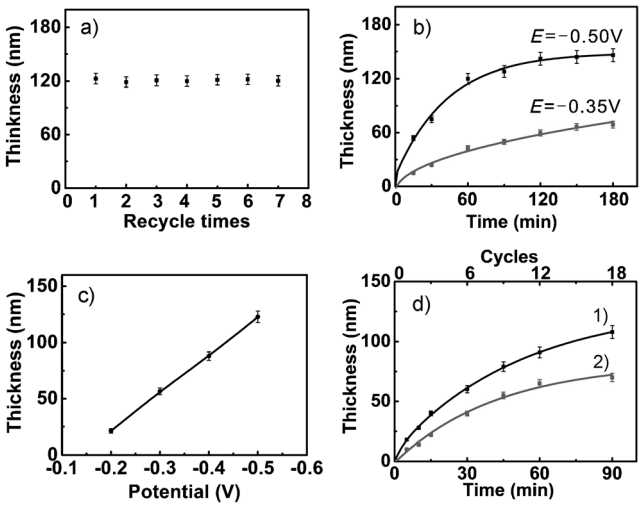

Figure 2. a) Recycling of the SPMA solution. PSPMA brushes grown from a Br-C15-thiol/2-NAT (20:1) electrode for 1 h. b) Linear first-order polymer growth at switched applied potentials. c) Ellipsometric polymer thickness of the PSPMA brushes grown on 20:1 Br-C15-thiol/2-NAT mixed SAMs at different applied potentials (reaction time 1 h). d) Kinetic plot of the PSPMA brushes grown on Br-C15-thiol/2-NAT (20:1) mixed SAMs at a square-wave potential, −0.5 V for 270 s and 0.4 V for 30 s (1), −0.5 V for 180 s and 0.4 V for 120 s (2). The experiment was repeated after a specified time.

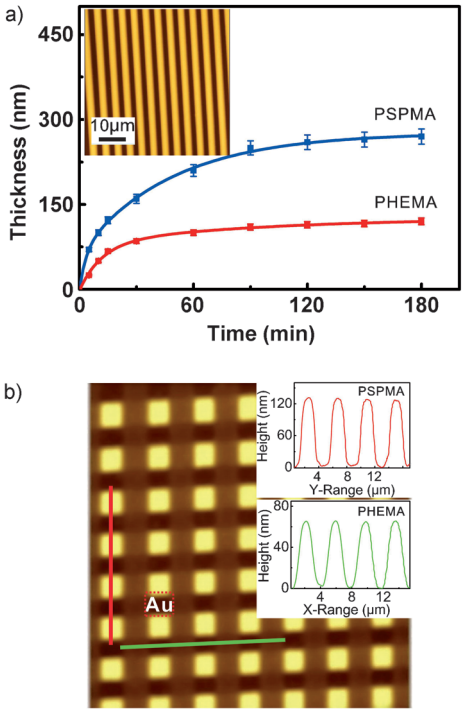

Figure 3. a) PSPMA (blue curve) and PHEMA (red curve) growth on Br-C15-thiol patterned gold surfaces. The inset is an AFM image of 260 nm thick PSPMA brushes. The reaction time was 2 h. b) AFM image of PSPMA and PHEMA crossed brushes, the reaction time was 0.5 h for HEMA and 2 h for SPMA. The insets are line traces showing the height of the PSPMA (top) and PHEMA (bottom) brushes, respectively.

aim of deactivating the chain growth rapidly and reducing the chance of chain termination. The growth of polymer brushes can be switched on and off. Figure 2d shows two cases in which one sample grew by applying an activation potential of −0.5 V for 270 s and a deactivation potential of 0.4 V for 30 s (curve 1), and −0.5 V for 180 s and 0.4 V for 120 s (curve 2). Both polymer brushes showed well-controlled growth of brushes in agreement with the length of the activation potential.

eATRP can also be used to form patterned brushes from Br-C15-thiol SAMs patterned through microcontact printing (μCP)[33] (Figure 3a). Here, no mixed Br-C15-thiol/2-NAT monolayer was required as parts of the gold surface are bare, and the brush growth was very fast and led to much thicker brushes. As shown in the inset, well-defined patterns with 260 nm thick PSPMA brushes were obtained (compared to 140 nm thick homogeneous brushes on 20:1 Br-C15-thiol/2-NAT-modified electrodes for the same grafting time). The living nature of eATRP can be displayed by copolymerization: after growing an 80 nm thick PHEMA brush, the sample was immersed in a second monomer solution to add a second 30 nm thick PSPMA block. The approach is also suitable for fabricating binary polymer brushes (i.e., surfaces containing two different polymer brushes) by two-step printing of an initiator monolayer.[33] After growing 66 nm thick PHEMA brushes from the first patterned initiator SAM, a cross-pattern is produced in a second printing step, followed by growth of 132 nm thick PSPMA brushes (Figure 3b). Clearly, eATRP allows polymer brushes to be prepared with controlled thickness, composition, and architecture.

It is illustrative to compare PSPMA brushes with similar thickness prepared by eATRP and conventional surface-initiated ATRP by swelling experiments and electrical impedance spectroscopy (EIS). Brushes grown by eATRP have a much larger swelling ratio ($h_{swollen}/h_{dry} = 3.83$) than those grown by a conventional approach ($h_{swollen}/h_{dry} = 1.77$; data in Figure S4 in the Supporting Information). As the swelling ratio of the polyelectrolyte brushes correlates linearly with the degree of polymerization,[34] these results indicate that the eATRP brushes have a higher molecular weight. As the brushes have very similar thickness (44 and 48 nm) the eATRP brushes must therefore have a lower grafting density. This conclusion is supported by the lower impedance measured on eATRP brushes (Figure S5 in the Supporting Information), which indicates less resistance to the diffusion of electroactive species through the brushes.

In conclusion, we have proven that electrically induced surface-initiated ATRP is an effective way to prepare polymer brushes of different types. The thickness of polymer brushes is controlled through adjusting the fraction of initiator and applied potentials. It allows polymer brushes to grow in the presence of ambient air and the monomer solution can be reused for several times, which is very promising for the polymerization of specialty monomers and for the growth of biocompatible, protein-resistant polymer brushes on nonplanar substrates with complex shapes.

Experimental Section

See the Supporting Information for details regarding the used materials and characterization methods.

Electrochemically mediated ATRP was initiated at a constant potential and continued for a certain time at room temperature to yield the electrode modified by polymer brushes. A typical eATRP polymerization takes place in a solution of bipy (122 mg, 0.78 mmol), $CuCl_2 \cdot 2H_2O$ (43 mg, 0.25 mmol), 3-sulfopropyl methacrylate potassium salt (SPMA) monomer (5.9 g, 24 mmol), and benzyltri-*n*-butylammonoim chloride (BBAC) supporting electrolyte (235 mg, 100 mM) in 7.5 mL solution of 2:1 (v/v) H_2O/MeOH. Polymerization of 2-hydroxyethyl methacrylate (HEMA): HEMA 3.1 g, bipy 122 mg, $CuCl_2 \cdot 2H_2O$ 43 mg, BBAC (100 mM),and H_2O/MeOH 2:1 (v/v).

Received: February 24, 2012
Published online: April 12, 2012

Keywords: polymerization · polymer brushes · surface chemistry

[1] S. Edmondson, V. L. Osborne, W. T. S. Huck, *Chem. Soc. Rev.* **2004**, *33*, 14.
[2] J. Pyun, K. Matyjaszewski, *Chem. Mater.* **2001**, *13*, 3436.
[3] M. A. C. Stuart, W. T. S. Huck, J. Genzer, M. Müller, C. Ober, M. Stamm, G. B. Sukhorukov, I. Szleifer, V. V. Tsukruk, M. Urban, F. Winnik, S. Zauscher, I. Luzinov, S. Minko, *Nat. Mater.* **2010**, *9*, 101.
[4] T. Chen, R. Ferris, J. Zhang, R. Ducker, S. Zauscher, *Prog. Polym. Sci.* **2010**, *35*, 94.
[5] H. Ma, J. Hyun, P. Stiller, A. Chilkoti, *Adv. Mater.* **2004**, *16*, 338.
[6] J. L. Dalsin, B.-H. Hu, B. P. Lee, P. B. Messersmith, *J. Am. Chem. Soc.* **2003**, *125*, 4253.
[7] Z. Zhang, S. Chen, S. Jiang, *Biomacromolecules* **2006**, *7*, 3311.
[8] H. Kanazawa, K. Yamamoto, Y. Matsushima, N. Takai, A. Kikuchi, Y. Sakurai, T. Okano, *Anal. Chem.* **1996**, *68*, 100.
[9] L. Sun, G. L. Baker, M. L. Bruening, *Macromolecules* **2005**, *38*, 2307.
[10] M. Ramstedt, N. Cheng, O. Azzaroni, D. Mossialos, H. J. Mathieu, W. T. S. Huck, *Langmuir* **2007**, *23*, 3314.
[11] F. Zhou, P. M. Biesheuvel, E.-Y. Choi, W. Shu, R. Poetes, U. Steiner, W. T. S. Huck, *Nano Lett.* **2008**, *8*, 725.
[12] F. Zhou, W. Shu, M. E. Welland, W. T. S. Huck, *J. Am. Chem. Soc.* **2006**, *128*, 5326.
[13] M. Chen, W. H. Briscoe, S. P. Armes, J. Klein, *Science* **2009**, *323*, 1698.
[14] I. E. Dunlop, W. H. Briscoe, S. Titmuss, R. M. J. Jacobs, V. L. Osborne, S. Edmondson, W. T. S. Huck, J. Klein, *J. Phys. Chem. B* **2009**, *113*, 3947.
[15] J. Pyun, T. Kowalewski, K. Matyjaszewski, *Macromol. Rapid Commun.* **2003**, *24*, 1043.
[16] A. K. Nanda, K. Matyjaszewski, *Macromolecules* **2003**, *36*, 1487.
[17] X.-S. Wang, S. F. Lascelles, R. A. Jackson, S. P. Armes, *Chem. Commun.* **1999**, 1817.
[18] D. M. Jones, W. T. S. Huck, *Adv. Mater.* **2001**, *13*, 1256.
[19] K. Matyjaszewski, H. Dong, W. Jakubowski, J. Pietrasik, A. Kusumo, *Langmuir* **2007**, *23*, 4528.
[20] A. J. D. Magenau, N. C. Strandwitz, A. Gennaro, K. Matyjaszewski, *Science* **2011**, *332*, 81.
[21] T. S. Hansen, J. U. Lind, A. E. Daugaard, S. Hvilsted, T. L. Andresen, N. B. Larsen, *Langmuir* **2010**, *26*, 16171.
[22] D. M. Jones, A. A. Brown, W. T. S. Huck, *Langmuir* **2002**, *18*, 1265.
[23] R. P. Janek, W. R. Fawcett, *J. Phys. Chem. B* **1997**, *101*, 8550.
[24] J. J. Gooding, F. Mearns, W. Yang, J. Liu, *Electroanalysis* **2003**, *15*, 81.
[25] V. Ganesh, V. Lakshminarayanan, *J. Phys. Chem. B* **2005**, *109*, 16372.
[26] C. Miller, M. Grätzel, *J. Phys. Chem.* **1991**, *95*, 5225.
[27] E. Sabatani, J. Cohen-Boulakia, M. Bruening, I. Rubinstein, *Langmuir* **1993**, *9*, 2974.
[28] V. L. Osborne, D. M. Jones, W. T. S. Huck, *Chem. Commun.* **2002**, 1838.
[29] N. V. Tsarevsky, K. Matyjaszewski, *Chem. Rev.* **2007**, *107*, 2270.
[30] J. Queffelec, S. G. Gaynor, K. Matyjaszewski, *Macromolecules* **2000**, *33*, 8629.
[31] J. Qiu, K. Matyjaszewski, L. Thouin, C. Amatore, *Macromol. Chem. Phys.* **2000**, *201*, 1625.
[32] N. Bortolamei, A. A. Isse, A. J. D. Magenau, A. Gennaro, K. Matyjaszewski, *Angew. Chem.* **2011**, *123*, 11593; *Angew. Chem. Int. Ed.* **2011**, *50*, 11391.
[33] F. Zhou, Z. Zheng, B. Yu, W. Liu, W. T. S. Huck, *J. Am. Chem. Soc.* **2006**, *128*, 16253.
[34] Y. Tran, P. Auroy, L.-T. Lee, *Macromolecules* **1999**, *32*, 8952.

